Submitted to the Twenty-Eighth International Symposium on Combustion, Edinburgh, Scotland, 2000.

Near-Limit Flamelet Phenomena in Buoyant Low Stretch Diffusion Flames Beneath a Solid Fuel

by
S.L. Olson*
NASA Glenn Research Center, Cleveland, OH, USA

and

J.S. T'ien
Case Western Reserve University, Cleveland, OH, USA

*S. L. Olson
mail stop 500-115
NASA Glenn Research Center
Cleveland, OH 44135
phone (216) 433-2859
fax (216) 977-7065
sandra.olson@grc.nasa.gov

For Oral Presentation
Colloquium: Fire Research, Flame Spread, Fire Suppression

Total Word Count: 3602 + 2000 for 5 figures = 5602
(word processor count)

Near-Limit Flamelet Phenomena in Buoyant Low Stretch Diffusion Flames Beneath a Solid Fuel

by
S.L. Olson
NASA Lewis Research Center

and

J.S. T'ien
Case Western Reserve University

Abstract

A unique near-limit low stretch multidimensional stable flamelet phenomena has been observed for the first time which extends the material flammability limit *beyond* the one-dimensional low stretch flammability limit to lower burning rates and higher relative heat losses than is possible with uniform flame coverage. During low stretch experiments burning the underside of very large radii (≥75cm *stretch rate* ≤ 3 s^{-1}) cylindrical cast PMMA samples, multidimensional flamelets were observed, in contrast with a one-dimensional flame that was found to blanket the surface for smaller radii samples (higher stretch rate). Flamelets were observed by decreasing the stretch rate or by increasing the conductive heat loss from the flame. Flamelets are defined as flames that cover only part of the burning sample at any given time, but persist for many minutes. Flamelet phenomena is viewed as the flame's method of enhancing oxygen flow to the flame, through oxygen transport into the edges of the flamelet. Flamelets form as heat losses (surface radiation and solid-phase conduction) become large relative to the weakened heat release of the low stretch flame. While heat loss rates remain fairly constant, the limiting factor in the heat release of the flame is hypothesized to be the oxygen transport to the flame in this low stretch (low convective) environment. Flamelet extinction is frequently caused by encroachment of an adjacent flamelet. Large-scale whole-body flamelet oscillations at 1.2-1.95 Hz are noted prior to extinction of a flamelet. This oscillation is believed to be due a repeated process of excess fuel leakage through the dark channels between the flamelets, fuel premixing with slow incoming oxidizer, and subsequent rapid flame spread and retreat of the flamelet through the premixed layer. The oscillation frequency is driven by gas-phase diffusive time scales.

Introduction

Theoretical models of a one-dimensional stagnation-point diffusion flame predict radiative extinction at low stretch [1,2], where radiative heat loss becomes large relative to reduced heat release rates, and the flame quenches. Because it is difficult to obtain sufficiently low stretch rates in the presence of normal gravity buoyant flow in typical laboratory-scale flames, the low stretch extinction limit was only recently experimentally verified in drop tower microgravity experiments [3]. In [3], using a pure gaseous diffusion flame with reactants issuing from opposed tubes, a quenching limit at low stretch and a U-shaped flammability boundary with fuel percentage and stretch rate as coordinates was experimentally demonstrated. However, because of the limited microgravity time in the drop tower (10 s), the reactants' feed tube diameter (2 cm) and the spacing between the fuel and oxidizer tubes (1.5-2.5 cm) had to be kept small enough so the flame response time was fast enough to achieve a steady flame in the available microgravity time.

Due to these restrictions, two questions may be raised regarding the interpretation of the experimental results of [3]. First, how much heat did the flame lose to the feed tubes, since low-stretch flames are physically thick and the tube spacing was close? (i.e., heat losses are not from gas radiation alone). Second, since the lateral extent of the flame is small (flame diameter is approximately equal to the tube diameter), and the flame radius to flame zone thickness ratio is not much greater than unity, can the experiment be considered a truly one-dimensional flame? Theoretical models [1-3] assume one-dimensionality. To check the validity of the one-dimensional prediction of the low stretch extinction and the possibility of a non-one-dimensional extinction mode, a large scale flame experiment capable of producing truly one-dimensional flames is needed.

Large scale experiments were conducted burning the underside of flat PMMA disks [4], but it is difficult to characterize the stretch rate in this geometry. In addition, cellular instabilities were reported for samples larger than 8 cm in diameter. These cellular instabilities are quite

different from those reported in this paper, and are believed to be due to the finite flat geometry of the samples in the study.

In the present work, a large scale experiment has been carried out by burning the bottom surface of a cylindrical solid fuel (polymethylmethacrylate, PMMA) in normal gravity. In [2], it was demonstrated theoretically that the shape and location of the extinction boundary, as well as a number of important flame characteristics are almost identical for buoyant and forced convective environments. Applying the buoyant stretch rate $a \propto (g/R)^{1/2}$, where g is the gravitational constant and R is the radius of curvature of the solid fuel, we can study low stretch extinction phenomena in normal gravity by using a solid fuel of very large radius of curvature.

Estimation and Discussion of Relevant Scales

Before the experiment and results are presented, a discussion of several relevant length and time scales will be given. The energy balance at the solid-gas interface can be expressed by

$$\lambda_g \frac{dT_g}{dy} + q''_{rad} = \lambda_s \frac{dT_s}{dy} + \dot{m}'' L_v + \epsilon\sigma(T_s^4) \qquad (1)$$

where the first and second terms on the left side of Eqn. (1) are the rates of heat conduction and radiation from the gas, respectively. The first term on the right side is the rate of heat conduction into the solid, the second term is the rate of energy used for pyrolysis (vaporization), and the last is the rate of surface radiative loss. In theory, if steady burning is achieved [1,2], the solid phase temperature profile can be determined, and the thermal depth is α_s/r (where α_s is the solid thermal diffusivity, assumed to be constant (1.2×10^{-3} cm^2/s), and r is the regression rate of the solid). In this case, the surface temperature gradient is

$$\frac{dT_s}{dy}\Big|_s = (T_s - T_\infty)\ (r/\alpha_s) \qquad (2)$$

However, in low stretch flames, the linear burning rate r is very small, so the solid thermal depth is very large - larger than the solid-sample thicknesses typically used in experiments. In these experiments, *the solid (2.4 cm thick) is not truly thermally thick.* At large times, when the thermal wave reaches the back side of the solid sample, the thermal condition on the back surface of the sample (T_∞) becomes relevant.

The solid phase time scale for thermal wave penetration (heat up transient) to the back side is ℓ^2/α_s, where ℓ is the solid thickness (for a thick solid, the timescale is α_s/r^2). For a solid sample thickness of 2.4 cm, this time is 80 minutes. Before this time is reached, but after the ignition stimulant is removed, the solid thermal penetration continues and the in-depth conduction term in Eqn. (1) decays with time. From the perspective of the gaseous flame, as time progresses, less heat is "lost" into the solid and a stronger flame develops. However, as time progresses, surface regression reduces the sample thickness so that the penetration time is reduced and the thermal condition on the back surface of the sample becomes relevant, steepening the temperature gradient as the sample continues to regress. Thus the finite solid has two transients; the initial heat up as the thermal wave penetrates and heat losses are reduced, and the regression transient, as sample regresses and the back surface boundary condition moves closer to the burning surface, increasing the heat losses.

The *gaseous flame zone thickness* is related to the stretch rate a. The flame standoff distance is estimated to be either $(\alpha_g/a)^{1/2}$ or $(D_f/a)^{1/2}$, where α_g is the average gas thermal diffusivity, D_f is the average fuel vapor mass diffusivity, and a is the stretch rate. For low stretch diffusion flames (say at a=3 s^{-1}), this standoff distance is approximately 0.75 cm[5]. Since the flame thickness is two or three times greater, the characteristic gas length scale (flame zone thickness) is approximately 2 cm. To have an approximate one-dimensional flame, the flame width (lateral extent) must be an order of magnitude greater (~20 cm).

The characteristic gas phase time scale is ℓ_g^2/α_g, which is proportional to $1/a$. For a = 1.8-3 s^{-1} (flamelet regime), this time scale is of the order of a second. For events where

significant changes in the solid phase occur on the order of many minutes, the gas-phase may be considered quasi-steady, but the solid-phase is still unsteady.

Experiments

Normal gravity experiments were conducted with a buoyant stagnation point flame stabilized beneath a cylindrical cast PMMA fuel sample, shown in Figure 1. The stretch rate, a, is equal to $((\rho_e-\rho^*/\rho_e)\ g/R)^{1/2}$, where g is the gravity, R is the radius of curvature of the fuel sample, and the ρ ratio term is the normalized density difference between ambient (e) and average flame conditions(*). The stretch rate was varied by varying the radius of curvature from 2.5 cm to 200 cm, corresponding to stretch rates of 16.2 to 1.8 s^{-1}, respectively. The exposed burning area of the samples with $R \geq 20$ cm was 20 cm x 20 cm, with inert extensions on all sides to continue the cylindrical geometry beyond the burning area to minimize edge effects. The maximum flame standoff distance observed in the experiments was 0.75 cm, so the aspect ratio of the low stretch experiments was 10, as discussed above, to achieve a truly one-dimensional flame. With this geometry it is possible to conduct low stretch experiments at normal gravity that simulate the low stretch extraterrestrial environments of spacecraft, the Moon, or Mars.

Diagnostics included video recording of the flames from two views: a side view of the cylindrical geometry, for flame standoff distance measurements(100 pixels/mm), and a bottom surface view to image the flamelets (at a slightly oblique angle to avoid dripping molten PMMA on the camera). An infrared (0.6-15 microns) Schmidt-Boelter thermopile radiometer (0-0.2 W/cm^2) was positioned beneath one corner of the sample, and the reading was converted to W/cm^2 emitted from the sample+flame using an appropriate view factor. Additional detail on the experimental setup is reported elsewhere [5,6].

Models predict that quenching extinction is caused by excessive heat losses relative to heat release rates [1,2]. It is thus feasible that quenching extinction can be experimentally observed by 1) reducing the stretch rate to reduce the oxygen supply, which reduces the heat

release rate; 2) increasing the heat losses from the system, such as increasing the solid conduction term in Eqn. (1) (in addition to the intrinsic radiative loss term); or 3) a combination of 1) and 2). In these experiments, decreasing the stretch rate is accomplished by increasing the radius of curvature of the sample. Increasing the heat losses from the gaseous flame is accomplished in three ways. First, at early times in the experiment heat losses are high due to the inherently unsteady solid-phase, where the thermal wave has not yet penetrated throughout the solid and the subsurface solid heat conduction is greater than it would be for steady state for an infinitely thick sample. Second, at later times in the experiment heat losses again increase due to an inherent increase in solid conductive heat loss, which occurs as the surface regresses for the finite thickness sample. At intermediate times, a minimum in the heat loss occurs. Lastly, in addition to these inherent solid phase variations, the conductive heat loss can be manually changed by changing the back surface temperature boundary condition on the solid sample (using air, ice, and dry ice). This back surface boundary condition has been used as an initial condition for the test, or a step change in the condition during a test.

When the back surface is exposed to an ice bath as an initial condition, one-dimensional flames persist for stretch rates all the way down to 3.6 s^{-1}. At a=3 s^{-1} (R=75 cm), flamelets are observed throughout the test (100 minutes) with an ice bath. When the back surface of this same 75 cm sample was changed to air (a good insulator) as an initial condition, the flamelets are observed for a period of 55 minutes before transition to a one-dimensional flame. This time corresponds to the thermal penetration time for the regression-thinned sample (2.0 cm). The one-dimensional flame lasted for approximately 35 minutes and then reverted back to flamelets (see Fig. 2). Since the stretch rate stays constant during the test, the occurrence of the initial flamelets is due to the large subsurface conductive flux into the solid (the first term on the right hand side of Eqn.(1)) right after ignition. The large flux to the solid lowers the flame temperature (confirmed with thermocouple readings [5]) and weakens the flame, as discussed in the previous section. When the solid thermal wave extends through the solid, the subsurface conductive loss from the flame decreases and a one-dimensional flame can be reached. The strongest one-dimensional flame is inferred to occur at 65-70 minutes after ignition, when the flame standoff

distance and flame radiation readings peak in Fig.2. The ratio of heat loss (conductive and surface radiative flux terms in Eqn.(1)) to heat flux from the flame to the solid (left hand side of Eqn.(1)) has been estimated [5,6] to be 85% for this limiting one-dimensional flame. After this time, heat losses increase again due to the reduction of the sample thickness due to surface regression. At 90 minutes, the backside loss becomes great enough and the one-dimensional flame reverts back to flamelets. The one-dimensional flammability limit is thus determined to occur at a stretch rate of $3s^{-1}$.

Tests with 100 and 200 cm radius of curvature samples were performed where dry ice (-78.5°C sublimation) was used instead of an ice bath. However, the dry ice was added 30 minutes after ignition, a step change in the back surface boundary condition during the test, to avoid ignition limitations. The intent was to determine if increasing the conductive heat losses in-depth would be sufficient to quench the flamelets established over 100 and 200 cm radius of curvature samples. Changing from ice to dry ice is estimated to increase the steady-state solid conductive losses by more than 20%. After dry ice application, as in-depth conduction increased, the flamelets weakened, and flamelet coverage reduced. While the 100 cm sample's flamelets persisted even 95 minutes after the addition of the dry ice, the 200 cm sample's flamelets extinguished 45 minutes after the addition of dry ice, so extinction was achieved with the increased heat loss at a stretch rate of $1.8\ s^{-1}$. Thus as heat loss rates continue to increase relative to the heat release rates, flamelets extinguish.

Another interesting test is to increase the stretch rate during a test. In selected flamelet experiments, the low stretch buoyant flow was augmented briefly by a fan-blown forced flow to elevate the stretch rate via a mixed buoyant-forced flow [2]. This increased the heat release rate, and, as anticipated, uniform flame coverage was achieved during the elevated stretch period. Once the forced flow was turned off, however, the flame reverted back to flamelets, indicating that the flamelet phenomena is the natural state for very low stretch flames.

Flamelet Phenomena

A Description of Flamelets

Flamelets are defined here as flames that cover only part of the burning sample at any given time. The onset of flamelets is interpreted as the quench limit for a one-dimensional flame. The flamelet phenomena *extends* the material flammability beyond the one-dimensional flame extinction limit by increased local oxygen flux to the flamelet through the quenched channels.

The transient formation of flamelets after ignition can be seen in Figure 3. Just after ignition, full flame coverage is present, as shown in Figure 3a for a 75 cm radius sample. The flame develops holes (Fig. 3b) within about 30 seconds of ignition deactivation, which proceed to grow and dynamically tear the flame apart into flamelets (Fig. 3c,d). These holes have been theorized to be caused by a reduction in the local Damkohler number (ratio of characteristic local residence time to local chemical time) below a critical value [7]. The flame breakup period is characterized by rapid flame flashes across the burning sample, flamelet oscillations, and flamelet extinction. Approximately 1 minute after breakup commences, the flamelets "stabilize" below the surface (Fig.4a) and begin more leisurely meandering about the surface on a solid-phase timescale of minutes.

Since the low stretch diffusion flame beneath the solid fuel is oxygen-limited, flamelet phenomena at very low stretch, where the flame breaks up into pieces and becomes multi-dimensional, is viewed as the flame's method of enhancing oxygen flow to the flame, through oxygen transport into the edges of the flamelet. The minimum quenched channel width observed is about 2 cm (see Fig. 3d or Fig. 4a). This is of the same order as the flame zone thickness, which is also the characteristic gas diffusion length. With additional oxygen diffusion at the edges of flames, numerical calculations show a smaller flame standoff distance [8,9] as the stoichiometric flame location shifts toward the fuel surface. Figure 2 shows that, indeed, the flame standoff distance in the flamelet stages are smaller than the one-dimensional flame.

The shapes of flamelets are not entirely regular; they slowly (in time scales of many minutes) change in shape, with length to width aspect ratios of 1-2. Flamelets meander around the burning surface on time scales of tens of minutes (i.e. solid-phase time scales). During a test, the flamelets tend to grow and contract, spread and split into two. The flamelets cover every part of the sample during some part of the burn. The "channel" spacing between flamelets generally increases with decreasing stretch rate, as shown in Figure 4, although error bars are large on the spacing due to the unsteady nature of the flamelet phenomena. For 100 cm samples (Fig. 4b) , flamelets are on the order of 5-8 cm apart. For 200 cm samples (Fig. 4c), between one and two flamelets are stable at any given time. Unlike previous runs, which were able to show local soot spots around suspended droplets, these flamelets are all blue, with locally brighter spots where fuel vapor jets are being released. The typical cycle of the stable flamelet would be to grow in size and then split into two. The two would move apart, but one of the two would invariably extinguish and the cycle would repeat itself. Thus it seems that for this size sample (20cm x 20cm), there is no "stable" spacing for two adjacent flamelets for 200 cm radii samples. This is similar to phenomena observed in fingering instabilities for flame/smolder spread problems [10,11], where the spacing between fingers is a strong function of the incoming flow. These experiments also show that there is a minimum flamelet size on the order of 5 cm in radius, below which the flamelet will extinguish.

Flamelet Oscillations

Flamelets locally quench as they interact strongly with adjacent flamelets. One flamelet's hydrodynamic flow field can interfere with another's and the weaker flamelet becomes unstable. The local quenching is at times preceded by a period (typically on the order of a minute) of large-scale oscillations of the weaker flamelet. Figure 5 shows the oscillations of the edge of one such flamelet, which developed large-scale oscillations that continued for 30 seconds prior to quench (large scale in the sense that the oscillatory amplitude is of the same order as the flamelet size). This particular flamelet was larger initially, but had shrunken due to influence of a growing flamelet adjacent to it. The flamelet began flashing back over the

previously occupied area. This flashback was oscillatory in nature. During the expansion portion of each oscillation, the flamelet propagates through a premixed fuel/oxidizer zone. The flamelet edge speed during this portion of the cycle is extremely fast, typically in excess of 50 cm/s and accelerating, due to both the premixed flame speed and thermal expansion.

The oscillation frequency is measured from Figure 5 by taking the times that the cycle reaches its low point and plotting them as a function of oscillation number. This data is shown on the right axis of Figure 5. The frequency of this oscillation is measured to be 1.2 Hz, based on the slope of the data. The range of frequencies measured in flamelet tests was 1.2-1.95 Hz. The steadiness of the oscillations can also be observed to be quite good from this figure, showing only slow fluctuations around this steady frequency. This frequency is consistent with gas-phase characteristic times of approximately 1 second (ℓ_g^2/α_g).

Oscillations prior to local flamelet extinction were observed in every flamelet run. This resembles the near-limit candle flame oscillations [12,13]. Recent theories have attributed the oscillations to flame front heat and mass imbalance due to radiative heat loss and/or large fuel Lewis number [14,15]. Both criteria appear to be met for these experiments; oxygen supply is limited (limited heat release), heat loss rates are high relative to the heat release rate, and the fuel in this study, PMMA (molecular weight 100), has a Lewis number that is larger than unity.

Conclusions

Flamelets are a unique near-limit low stretch stable flame adaptation *observed for the first time* in this geometry for stretch rates below 3 s^{-1}. Flamelets are defined as flames that cover only part of the burning sample at any given time, but persist for many minutes. The flamelet burning regime extends the flammability of the material *beyond* the one-dimensional flame limit to lower burning rates and higher relative heat losses than is possible with uniform flame coverage. Flamelet phenomena is viewed as the flame's method of enhancing oxygen flow to the flame, through oxygen transport into the edges of the flamelet.

These experiments have demonstrated that flamelets can form either by decreasing the stretch rate or by increasing the conductive heat loss from the flame (in addition to intrinsic radiative loss). Since low stretch flames are thick, only a flame with sufficiently large lateral extent can display the flamelet phenomena. In adapting a large solid fuel for this purpose, however, we introduce an additional solid timescale which is very long, and the system is not truly steady when measured in this timescale. The slow meandering motion and the growth and contraction of flamelets may be the result of the inherent solid unsteadiness. It would be interesting to carry out the experiment with steady boundary conditions imposed (such as with a large scale purely gaseous flame) to see whether flamelets can be stationary and steady.

While the one-dimensional stagnation point theory has been instrumental and useful in the study of low stretch flame behavior, the inclusion of a flamelet regime will require an extension to multi-dimensional models.

References

1 T'ien,J.S.; *Combustion and Flame* 65, pp.31-34, 1986.

2 Fouch,D.W.,and T'ien,J.S.; *AIAA Journal*, Vol.25, No.7, pp.972-976, 1987.

3 Maruta,K.,Yoshida,M.,Guo,H.,Ju,Y.,and Niioka,T.; *Combustion and Flame* 112, pp.181-187,1998.

4 Vantelon,J.P., Himdi,A.,and Gaboriaud,F.; *Combustion Science and Technology* 54, pp.145-158, 1987.

5 Olson,S.L.; Ph.D. Dissertation, Case Western Reserve University,1997.

6 Olson,S.L.and T'ien,J.S.;, *Combustion and Flame*,to appear,2000.

7 Nayagam,V.,Balasubramaniam,R.,and Ronney,P.D.; *Combustion Theory and Modelling* 3,pp.727-742,1999.

8 Mell, W.E,and Kashiwagi,T., *Twenty-Seventh Symposium (International) on Combustion*, The Combustion Institute, pp.2635-2641, 1998.

9 Shih,H-Y.; PhD Dissertation, Case Western Reserve University, expected Jan. 2000.

10 Olson,S.L.,Baum,H.R.,and Kashiwagi,T.; *Twenty-Seventh Symposium (International) on Combustion*, The Combustion Institute, pp.2525-2533,1998.

11 Zik,O.,Olami, Zeev,and Moses,E.; *Physical Review Letters*, Vol.81, No.18,pp.3868-3871,1998.

12 Dietrich,D.L.,Ross,H.D.,and T'ien,J.S.;, AIAA 34th Aerospace Sciences Meeting, AIAA-94-0429,1994.

13 Chan,W.Y,and T'ien.J.S.; *Combustion Science and Technology* 18, pp. 139, 1998.

14 Cheatham,S.and Matalon,M.; *Twenty-Sixth Symposium (International) on Combustion*, The Combustion Institute, pp.1063-1070,1996.

15 Buckmaster,J., and Zhang,Y.; *Combustion Theory and Modelling* 3, pp.547-565,1999.

Figure Captions

Figure 1: schematic of a buoyant low stretch one-dimensional diffusion flame established in the stagnation flow region beneath a cylindrical solid fuel. In this cylindrical geometry, the stretch rate is proportional to $(g/R)^{1/2}$. The radius of curvature, R, was as large as 200 cm in the experiments.

Figure 2: flame standoff distance (solid line) and radiometer readings (dashed line) during a low stretch (a=3 s^{-1}) experiment with air as the back surface boundary condition. Both sets of data show the long-term solid-phase heat up and regression transients, while the gas-phase flame standoff distance reaches a fairly stable value during the 1-D uniform flame phase. The radiometer reading does not stabilize, but continually varies as the sooting character of the flame continually varies, maximizing between 55-75 minutes. Surface radiation alone is estimated to be 0.8 W/cm_2. "Noise" in each signal is actual variations of the flame; both readings detect the perturbations caused by frequent bubble rupture and vapor jetting from the surface. Dripping late in the test made flame standoff distance measurements impossible at times. The experiment was manually terminated at 118 minutes.

Figure 3: Dynamic flame breakup of a post-ignition uniform flame into flamelets: images are 5 seconds apart. View is slightly oblique.
a) post-ignition uniform flame over 20 cm x 20 cm sample viewed from below, showing local reaction thinning but flame still fully covers surface;
b) holes develop in flame sheet, with definite edges and downstream enhanced reaction;
c) holes grow and merge to form transient channels as the flame destabilizes over the sample;
d) channels become more stable, with a characteristic 2-3 cm spacing between flamelets.

Figure 4: flamelets stabilized beneath samples for stretch rates of a) 3 s^{-1}, b) 2.5 s^{-1}, and c) 1.8 s^{-1}. Oblique view is same as Figure 3.

Figure 5: Oscillating flamelet edge position as a function of time (line), showing oscillations for a flamelet beneath a 75 cm sample prior to local quenching of that flamelet. Tracking the low point in each oscillation (circles), the frequency of the oscillations is nearly steady until extinction at 1.2 Hz.

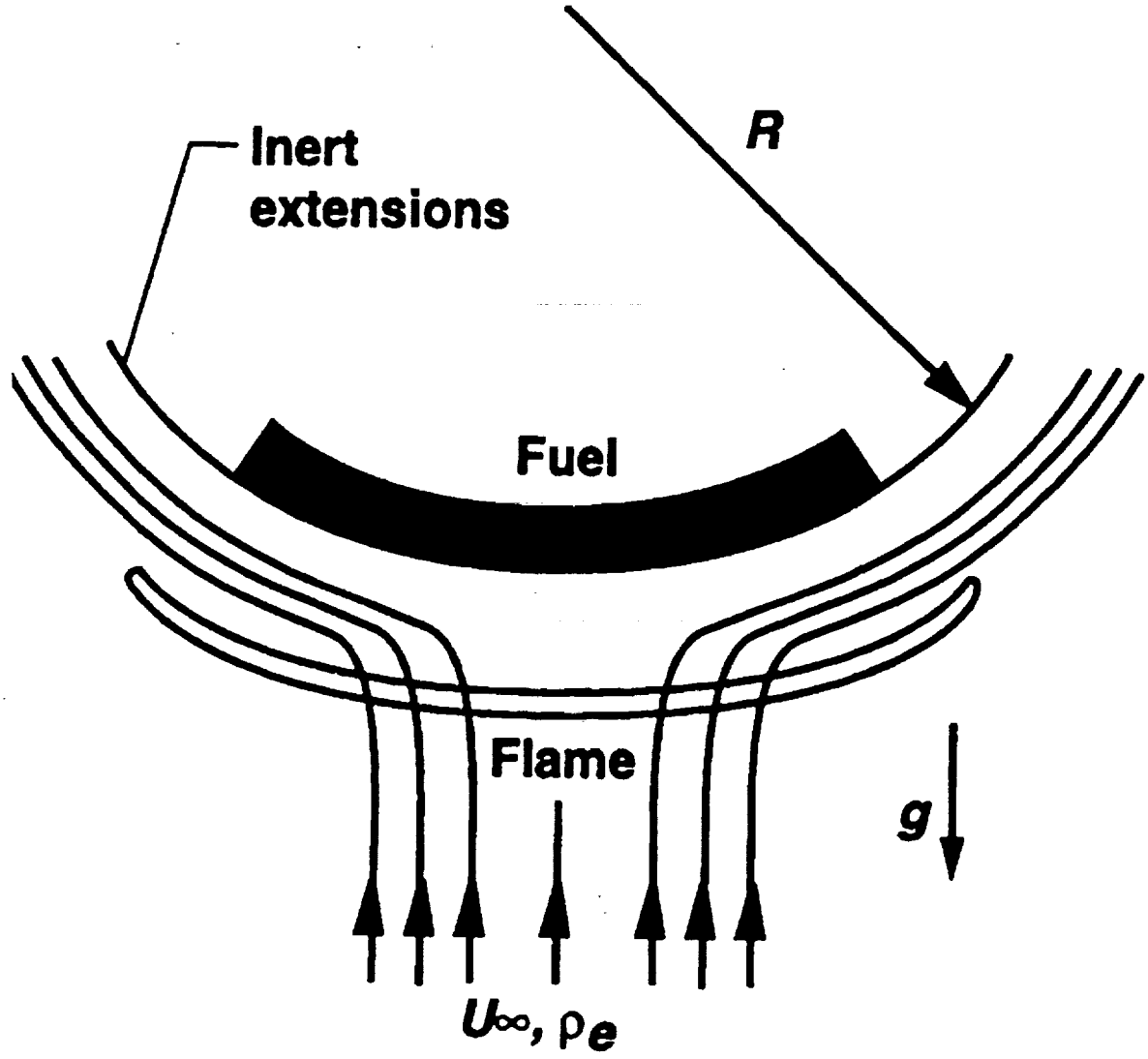
R
Inert
extensions
Fuel
Flame
g
U_∞, ρ_e

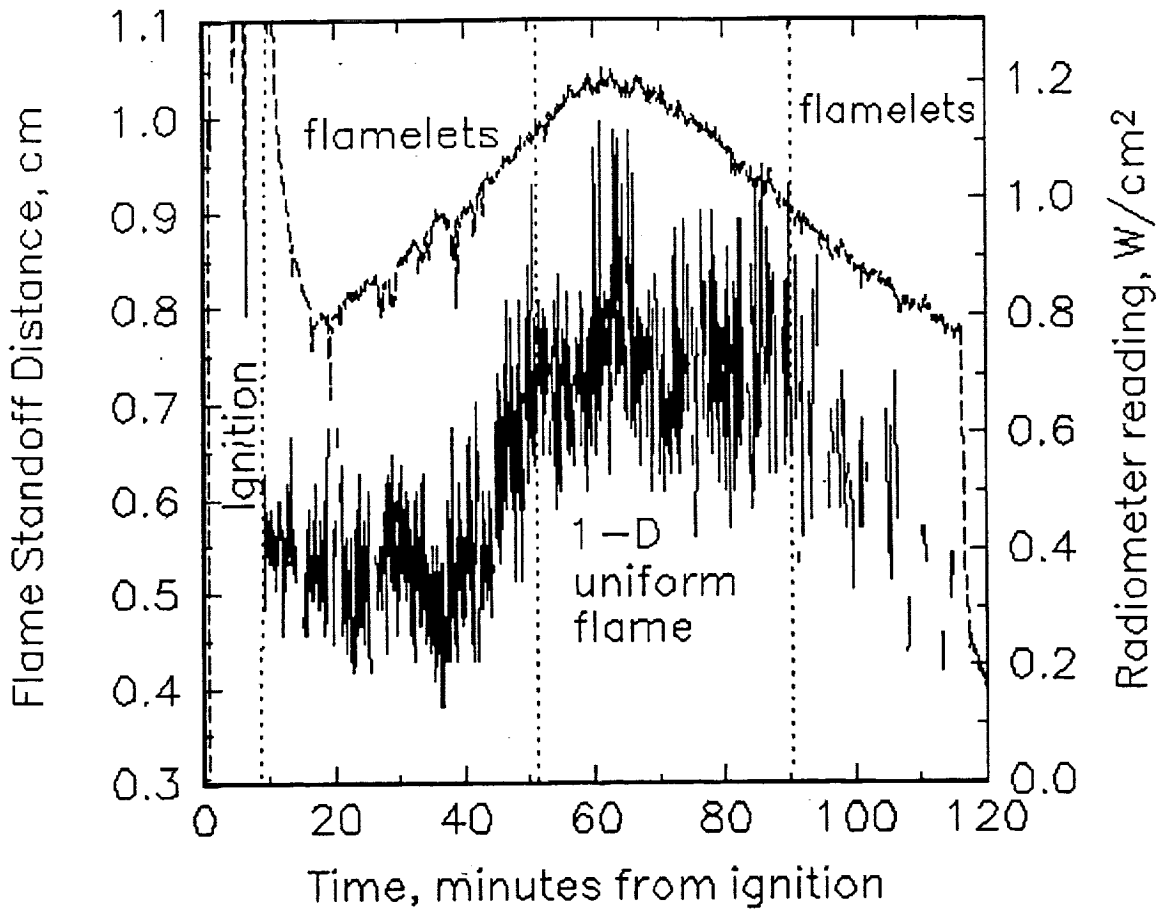
Flame Standoff Distance, cm
Radiometer reading, W/cm2
Time, minutes from ignition
flamelets
flamelets
Ignition
1 –D
uniform
flame
1.1
1.0
0.9
0.8
0.7
0.6
0.5
0.4
0.3
1.2
1.0
0.8
0.6
0.4
0.2
0.0
0
20
40
60
80
100
120

a)

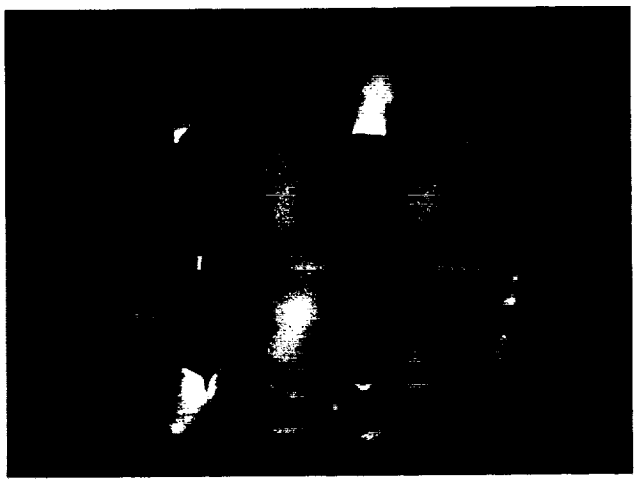

b)

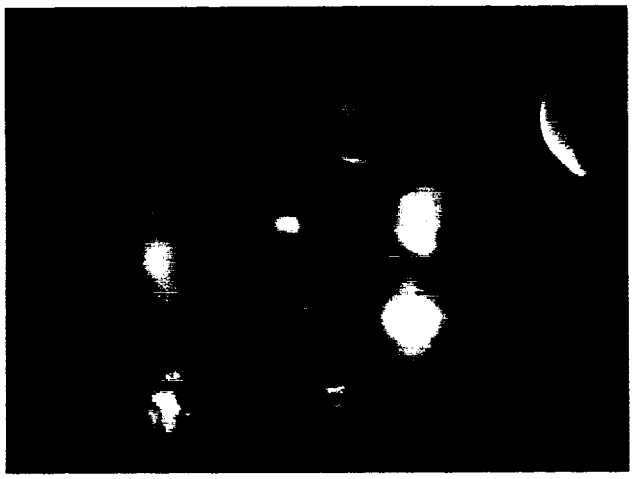

c)

d)

a)

b)

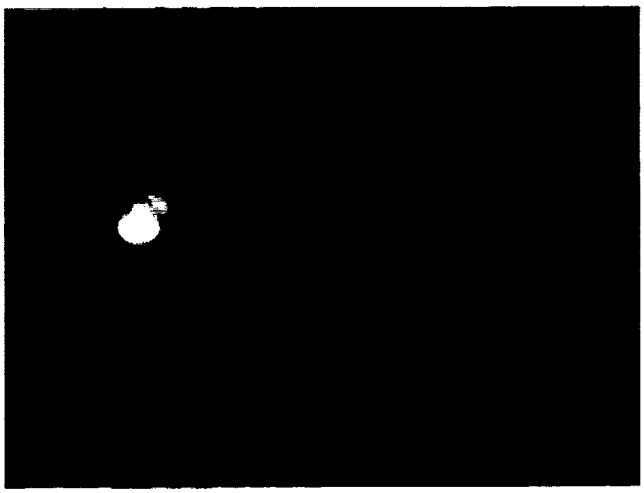

c)

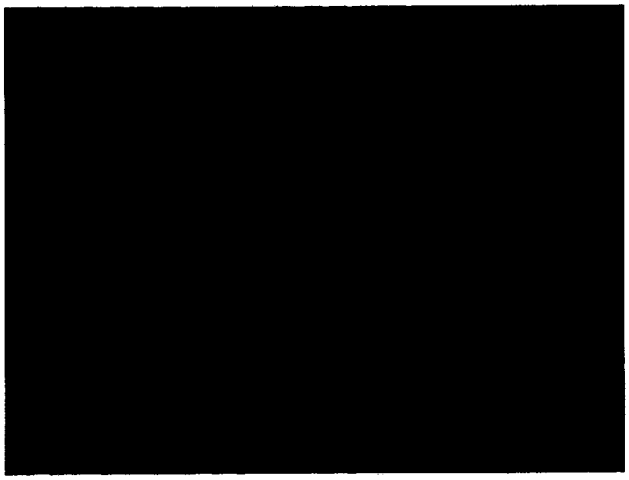

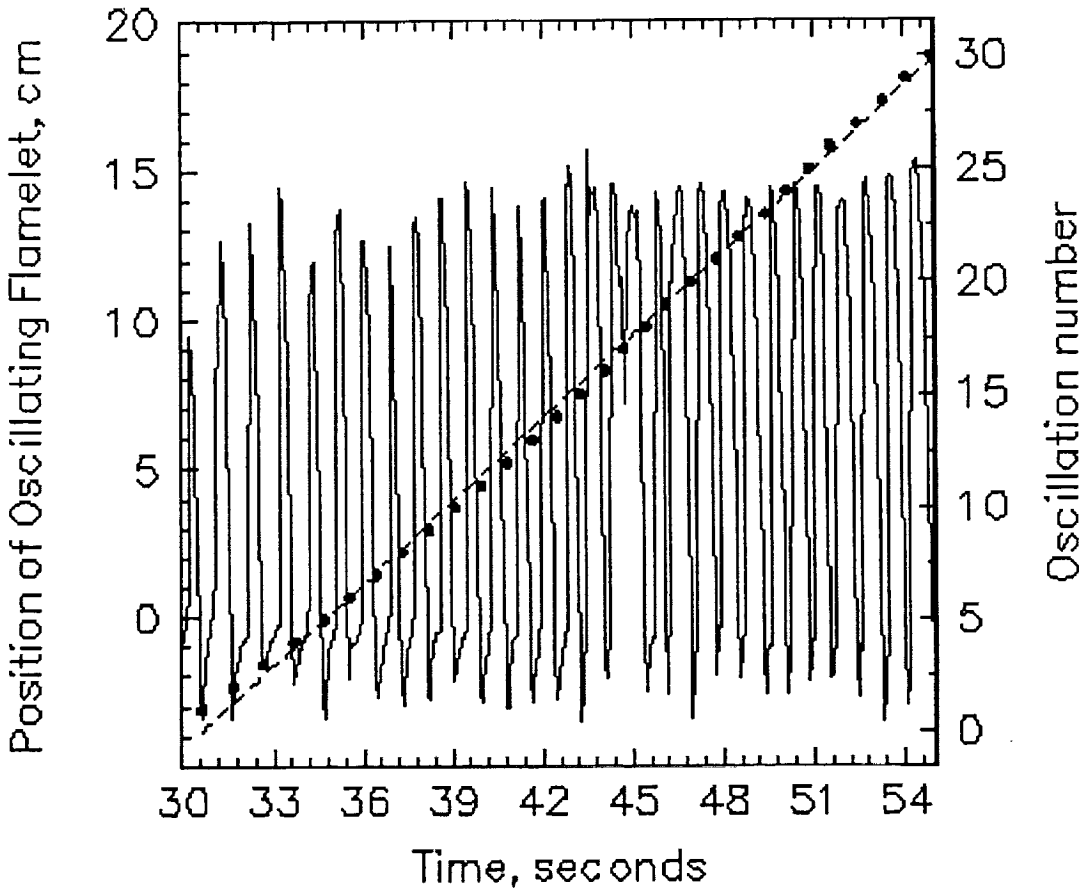
Position of Oscillating Flamelet, cm
20
15
10
5
0
30
25
20
15
10
5
0
Oscillation number
30 33 36 39 42 45 48 51 54
Time, seconds